

Determination of stellar parameters for S-PLUS stars through bayesian SED fitting

Guilherme Fabricio Bolutavicius¹, Felipe de Almeida-Fernandes^{1,2}, & Claudia Lucia Mendes de Oliveira¹

¹ Instituto de Astronomia, Geofísica e Ciências Atmosféricas da Universidade de São Paulo
e-mail: guilherme.bolutavicius@usp.br

² NSFs NOIRLab, Tucson, AZ
e-mail: felipe.almeida.fernandes@usp.br

Abstract. With the objective of determining atmospheric stellar parameters (Teff, logg and [Fe/H]) for stars observed by the Southern Photometric Local Universe Survey (S-PLUS), we fitted synthetic spectra from a spectral library to their magnitudes. The spectral grid, after being interpolated, is convoluted with the filters from S-PLUS and another reference catalog (e.g. SDSS). Utilizing a bayesian fitting, which takes into account both the χ^2 , between the synthetic and instrumental magnitudes, and a prior, calculated based on the distribution of stellar parameters of a simulated sample of stars (using MIST isochrones). The fit is usually done in two steps, given that it is also a calibration step for the instrumental magnitudes. The first stage is done using magnitudes from a reference catalog, while on the second stage, it is done using the S-PLUS filters that were just calibrated with the zero-points from the last step. We have observed that the usage of a prior is necessary in circumstances where the dust extinction (E_{B-V}) is also included as a fitting parameter, as it is expected some degeneracy between this and the effective temperature. We showed that using the prior is still beneficial in scenarios where the magnitudes are previously corrected using extinction maps. So far we were able to obtain temperatures with a -108K offset and standart deviation of 127K, in addition to a logg with -0.48 dex and 0.51 dex of offset and standart deviation, respectively, comparing the data with a LAMOST's DR5. Concerning the metallicity, the obtained offset was of 0.03 dex, while the standart deviation was approximately 0.34 dex. This values are referring to the STRIPE-82 region and some surrounding fields of the iDR4 of S-PLUS.

Resumo. Com o objetivo de determinar parâmetros estelares atmosféricos (Teff, logg e [Fe/H]) para estrelas observadas pelo Southern Photometric Local Universe Survey (S-PLUS), ajustamos espectros sintéticos de uma biblioteca espectral às suas magnitudes. O grid de espectros, depois de interpolado, é convoluído com os filtros do S-PLUS e de outro catálogo de referência (por exemplo, SDSS). Utilizando um ajuste bayesiano, que leva em conta tanto o χ^2 , entre as magnitudes sintética e instrumental, e um prior, calculado com base na distribuição de parâmetros estelares de uma amostra simulada de estrelas (usando isócronas MIST). O ajuste geralmente é feito em duas etapas, visto que também é uma etapa de calibração para as magnitudes instrumentais. O primeiro estágio é feito usando magnitudes de um catálogo de referência, enquanto no segundo estágio, é feito usando os filtros S-PLUS que foram calibrados com os zero-points do último passo. Observamos que o uso de um prior é necessário em circunstâncias em que a extinção por poeira (E_{B-V}) também está incluída como parâmetro de ajuste, pois é esperada alguma degenerescência entre esta e a temperatura efetiva. Mostramos que usar o prior ainda é benéfico em cenários onde as magnitudes são corrigidas previamente usando mapas de extinção. Até agora conseguimos obter temperaturas com offset de -108K e desvio padrão de 127K, além de um logg com -0,48 dex e 0,51 dex de offset e desvio padrão, respectivamente, comparando os dados com o DR5 do LAMOST. Em relação à metalicidade, o offset obtido foi de 0,03 dex, enquanto o desvio padrão foi de aproximadamente 0,34 dex. Esses valores são referentes à região STRIPE-82, e alguns campos próximos, do iDR4 do S-PLUS.

Keywords. Stars: fundamental parameters – Stars: atmospheres – Techniques: photometric

1. Introduction

The Southern Photometric Local Universe Survey (S-PLUS, Mendes de Oliveira et al. 2019) is a photometric survey that observes the southern sky using 12 photometric bands (Figure 1 of Almeida-Fernandes et al. 2022), among them there are 5 sloan-like broad-band filters (u, g, r, i, z) and 7 narrow-band filters (j0378, j0395, j0410, j0430, j0515, j0660, j0861), including filters that are sensitive to metallicity (like j0378, near the OII line) and log g (like j0515, on the region of the Mgb triplet).

As part of the S-PLUS calibration pipeline (Almeida-Fernandes et al. 2022), field stars go through a SED fitting process using spectral libraries like Coelho (2014). This is done in order to estimate the calibration zero-points (ZPs) with the difference between the model magnitudes and the instrumental ones.

Here we compare a bayesian fitting strategy with the χ^2 minimization method, we also apply an interpolated version of the

SED grid. For that we used some fields of the iDR4 of SPLUS (Figure 1).

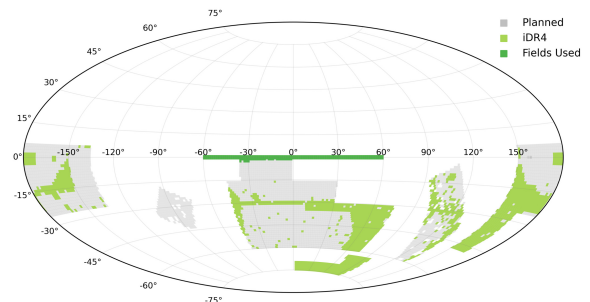


FIGURE 1. Footprint of S-PLUS. In grey are the planned fields to be observed, in light green are all the fields available in iDR4 and in dark green there are the fields used in this work.

2. Methods

As previously mentioned, the main idea, present in all scenarios analysed here, is to convolute the SEDs from Coelho (2014) with S-PLUS filters and use this model magnitudes to fit the parameters for the given star. We also use an interpolated grid of spectra, based on the previous (Figure 1 of Coelho 2014), in order to try to minimize errors (given that the models are discretized).

The first option is to use a simple χ^2 minimization between catalog (PStotal) S-PLUS magnitudes and the model magnitudes. In this project we used data already corrected for dust extinction (usign Schlegel et al. 1998) but it is worth noting that whenever the E_{B-V} is fitted, simultaneously with the other parameters, there is a very clear degeneracy between it and the effective temperature, which is diminished very well using the next method with bayesian fitting.

Another option, as mentioned above, is to use a bayesian-like fitting, where not only the χ^2 is taken into account, but also a prior probability for each triplet of atmospheric parameters (T_{eff} , $\log g$ and $[\text{Fe}/\text{H}]$).

In order to calculate the priors, without using distribution functions from observational data, we generated a series of simulated star samples. From these we smoothed the parameter distributions with kernel density estimators (KDEs) and used them as the prior for our method. In Figure 2 we show the prior distributions as a function of temperature and metallicity.

The samples were generated using MIST isochrones (Dotter 2016). We had the liberty to choose defining parameters for the sample, like an initial mass function and a star formation history. Among those there was the metallicity distribution, which is of key importance, as $[\text{Fe}/\text{H}]$ is one of the fitting parameters.

It is known that the usual metallicity distribution of Halo stars and Disk stars is different, and for that reason, the Halo Fraction (HF) is an important input for the $[\text{Fe}/\text{H}]$ distribution in the simulation. It is worth noting that this HF changes for each S-PLUS pointing. As a solution to that we defined several priors from samples generated with different HFs, in particular with 0.07, 0.20, 0.32, 0.42, 0.52 and 0.62. Then, for every field we determined the halo fraction using the TRILEGAL code (Girardi et al. 2005) and used the prior with the closest corresponding HF.

3. Results

Here we analysed 4 situations, covering aspects discussed in Section 2. In one case (A) we used the least square fitting, while on the others we used the bayesian fitting. Among these 3, in (B) we fixed the HF to 0.52 and on the others (C and D) we varied it according to the field, as mentioned previously. For the last one (D) we also interpolated the original SEDs.

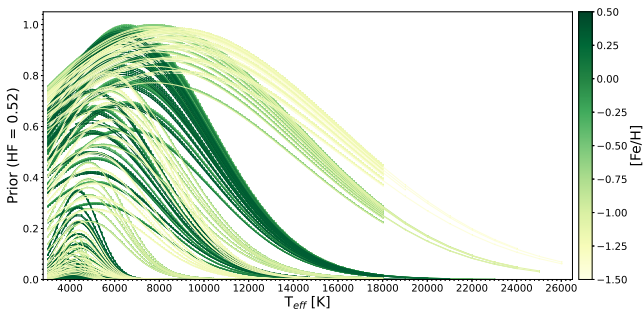


FIGURE 2. Prior distributions (for a halo fraction of 52%) in terms of the effective temperature and metallicity. The different curves represent different bins of $\log g$ and $[\text{Fe}/\text{H}]$.

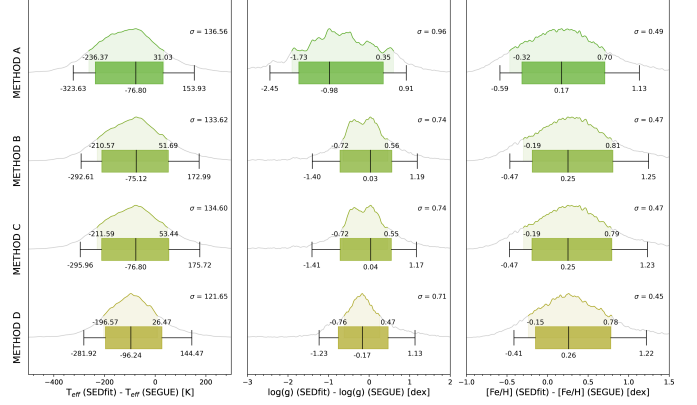


FIGURE 3. Comparing the 4 methods described in the text with data from SSPP. The bars on the left and right represent the 0.05 and 0.95 percentiles, while the box delimits the interval between 0.16 and 0.84. The line in the middle shows the mode of the distribution while the shadow on the profile shows the full width half maximum.

In Figure 3, we have a comparison between the methods by crossmatching the data with SSPP (Smolinski et al. 2011) stars. The most visible change is in $\log g$, which gains a lot with the bayesian fitting. All parameter reduced the width of the error distribution when using interpolation but not as much as expected. Another interesting aspect is that the difference between (B) and (C) are negligible for this dataset. We mainly expected a difference in $[\text{Fe}/\text{H}]$, but this result shows that the prior doesn't influence the metallicity fitting as much. Table 1 shows comparison results for the most complete method (D).

TABLE 1. Offsets and standart deviations (σ) when comparing the obtained values with SED fitting to SEGUE and LAMOST data.

Parameter	SED _{fit} - SEGUE		SED _{fit} - LAMOST ^a	
	offset	σ	offset	σ
T_{eff}	-96.24	121.65	-107.92	126.74
$\log g$	-0.17	0.71	-0.48	0.51
$[\text{Fe}/\text{H}]$	0.26	0.45	0.03	0.34

^a Recalibrated by G. Limberg (private communication).

4. Conclusion

We showed, for a region of SPLUS iDR4, the results for a bayesian fitting method to get the atmospheric parameters. The final method used both the interpolation of the models grid and the bayesian approach with priors from simulated samples. Comparing to SSPP we obtained, for T_{eff} , $\log g$ and $[\text{Fe}/\text{H}]$ respectively, modal errors of -96K, -0.17 dex and 0.26 dex and standart deviations of 122K, 0.71 dex and 0.45 dex.

References

- Almeida-Fernandes, F., et al., 2022. MNRAS, vol. 511, no. 3, pp. 4590–618.
Coelho, P. R. T., 2014. MNRAS, vol. 440, no. 2, pp. 1027–43.
Dotter, A., 2016. ApJ, vol. 222, no. 1, Jan., p. 8.
Girardi, L., et al., 2005. A&A, vol. 436, no. 3, pp. 895–915.
Luo, A.-Li, et al., 2015. RAA, vol. 15, no. 8, pp. 1095–124.
Mendes de Oliveira, C., et al., 2019. MNRAS, vol. 489, no. 1, pp. 241–67.
Schlegel, D. J., et al., 1998. ApJ, vol. 500, no. 2, pp. 525–53.
Smolinski, Jason P., et al., 2011. ApJ, vol. 141, no. 3, Feb. 2011, p. 89.